1003-7713/2004/03-292-13

利用真空紫外脉冲场电离-光电子方法研究三氯乙烯阳离子振动光谱

胡显冠， 刘佳聪， 伍灼耀**
（加利福尼亚大学戴维斯分校化学系，戴维斯市，加利福尼亚州，95616）

摘 要： 在 76400～79650 cm^{-1} 的能量范围内测量了三氯乙烯的真空紫外脉冲场电离-光电子（VUV-PFI-PE）谱. 根据量子化学理论计算的频率以及 Franck-Condon 因子，对 VUV-PFI-PE 谱的振动谱带进行了标定，确认了 11 个三氯乙烯阳离子的振动频率，分别为：$\nu_1^+ = 148\ cm^{-1}$，$\nu_2^+ = 180\ cm^{-1}$，$\nu_3^+ = 286\ cm^{-1}$，$\nu_4^+ = 402\ cm^{-1}$，$\nu_5^+ = 472\ cm^{-1}$，$\nu_6^+ = 660\ cm^{-1}$，$\nu_7^+ = 875\ cm^{-1}$，$\nu_8^+ = 990\ cm^{-1}$，$\nu_9^+ = 1038\ cm^{-1}$，$\nu_{10}^+ = 1267\ cm^{-1}$，$\nu_{11}^+ = 1408\ cm^{-1}$. 这些测量和新近用真空紫外-红外光诱导电离确定的 $\nu_{12}^+ = 3073\ cm^{-1}$ 一起，提供了三氯乙烯阳离子电子基态的所有 12 个振动频率的实验值. 通过对 VUV-PFI-PE 谱（0，0）跃迁带的光谱拟合，确定了三氯乙烯的电离能为（76441.7 ± 2.0）cm^{-1}（（9.4776 ± 0.0002）eV）.

关键词： 真空紫外脉冲场电离-光电子；三氯乙烯；振动光谱
中图分类号：O64 **文献标识码：**A

Vibrational Spectroscopy of Trichloroethene Cation by Vacuum Ultraviolet Pulsed Field Ionization-photoelectron Method*

Woo H K， Lau K C， Ng C Y**
（*Department of Chemistry*, *University of California at Davis*, *Davis*, *California* 95616）

Abstract The vacuum ultraviolet（VUV）pulsed field ionization-photoelectron（PFI-PE）spectrum for trichloroethene（$ClCH = CCl_2$）has been measured in the energy range of 76400～79650 cm^{-1}. The vibrational bands resolved in the VUV-PFI-PE spectrum are assigned based on *ab initio* vibrational frequencies and calculated Franck-Condon factors for the ionization transitions, yielding eleven vibrational frequencies for $ClCH = CCl_2^+$: $\nu_1^+ = 148\ cm^{-1}$, $\nu_2^+ = 180\ cm^{-1}$, $\nu_3^+ = 286\ cm^{-1}$, $\nu_4^+ = 402\ cm^{-1}$, $\nu_5^+ = 472\ cm^{-1}$, $\nu_6^+ = 660\ cm^{-1}$, $\nu_7^+ = 875\ cm^{-1}$, $\nu_8^+ = 990\ cm^{-1}$, $\nu_9^+ = 1038\ cm^{-1}$, $\nu_{10}^+ = 1267\ cm^{-1}$, and $\nu_{11}^+ = 1408\ cm^{-1}$. These measurements along with the frequency $\nu_{12}^+ = 3073\ cm^{-1}$ determined in the recent VUV-infrared photo-induced ionization study have provided the complete set of twelve experimental vibrational frequencies for $ClCH = CCl_2^+$ in its ground electronic state. On the basis of the spectral simulation of the origin VUV-PFI-PE vibrational band, we have determined the *IE*（$ClCH = CCl_2$）to be（76441.7 ± 2.0）cm^{-1}（（9.4776 ± 0.0002）eV）.

Keywords Vacuum ultraviolet pulsed field ionization-photoelectron, Trichloroethene, Vibrational spectroscopy

---

* Dedicated to the 80th birthday of Professor Qihe Zhu.

** Corresponding author, E-mail：cyng@ chem. ucdavis. edu Received 14 January 2004.

1 Introduction

Chlorinated ethenes, such as trichloroethene ($ClCH=CCl_2$), have been extensively used as industrial solvents. Because of its heavy usage, trichloroethene is known to be one of the persistent contaminants in soil and ground water[1,2]. For this reason, the chemical properties and reactivity of trichloroethene have been the subject of environmental studies[3-5]. Several studies on the photodissociation of trichloroethene have been reported[6-11]. Through the measurement of product translational energy distributions, information about the potential energy barriers, the bond dissociation energy, and the branching ratios for the HCl and Cl elimination channels has been obtained. The HeI photoelectron and photoionization efficiecncy (PIE) studies of $ClCH=CCl_2$ have been made. These studies report values in the range of 9.45 ~9.68 eV for the ionization energy (IE) of $ClCH=CCl_2$[12].

The pulsed field ionization (PFI) techniques[13-20], together with the development of vacuum ultraviolet (VUV) laser[21,22] and high-resolution monochromatized VUV synchrotron[23] sources, have played an important role in advancing the study of ion spectroscopy and chemistry[24]. The established high-resolution PFI-techniques include PFI-photoelectron (PFI-PE)[13-15] and PFI-photoion (PFI-PI)[16-18] for spectroscopic measurements, the PFI-PE-photoion coincidence[19] for unimolecular dissociation studies, and the PFI-PE-secondary ion coincidence schemes[20] for bimolecular reaction studies of ion-neutral collisions.

In the spectroscopy front, the analyses of rotationally resolved PFI-PE spectra have provided highly precise *IE* values and rotational constants for many simple molecules[24,25]. Nevertheless, the general energy resolution of about 1 cm^{-1} (full width at half maximum, FWHM) achieved for PFI-PE measurements is still insufficient for resolving individual rotational transitions involving polyatomic molecules, such as $ClCH=CCl_2$ in the present study. Despite the use of the supersonic beam method to cool the gas sample to a rotational temperature of ≈30 K, the FWHM of the origin PFI-PE band for a polyatomic molecule is still found to be in the range of 10 ~ 20 cm^{-1}. In an effort to obtain *IE* values with a higher precision than that limited by the FWHM of the origin band, we have developed a semi-empirical routine for the simulation of partially resolved rotational contours generally observed in the origin PFI-PE vibrational bands. Such simulations have shown to provide *IE* values with error limits well within ±2 cm^{-1} for simple polyatomic molecules[26-30]. Other than the *IE* value, PFI-PE and PFI-PI studies have become the major source of information about the vibrational spectroscopy of polyatomic ions. For single-photon VUV photoionization studies, the Franck-Condon factors (FCFs) involved can be calculated by *ab initio* quantum chemical procedures. The comparison between the VUV-PFI-PE or VUV-PFI-PI spectra and the FCF simulated spectrum have made possible the reliable assignment of vibrational bands resolved in the VUV-PFI-PE or VUV-PFI-PI spectra of many polyatomic molecules[29-32]. For two-color UV PFI-PE studies, the nature of the intermediate state is often not well known for a FCF simulation to be performed. Thus, the vibrational assignment of the PF-PE thus obtained is not as straight forward.

Although the VUV-PFI-PE and VUV-PFI-PI schemes are powerful techniques for spectroscopy studies of cations, these single-photon techniques have a limitation that many ion vibrational modes cannot be excited because of negligible FCFs for the photoionization transitions. It has been shown that high frequency vibrational modes involving the C – H, O – H, and N – H stretching motions, which are indiscernible in VUV-PFI-PE spectra, can be readily observed in infrared (IR)-photoinduced Rydberg ionization (PIRI) measurements[33-35]. Thus, the IR-PIRI method is complementary to the VUV-PFI-PE and VUV-PFI-PI techniques. We have recently demonstrated the first VUV-IR-PIRI study on $ClCH=CCl_2$ using tunable VUV and IR laser sources[35]. By first exciting $ClCH=CCl_2$ to a sufficiently high-n Rydberg state prior to the IR-PIRI measurement, we find that the IR-PIRI spectrum is independent of n for a broad range of $n \approx 10 \sim 93$. This observation indicates that the Rydberg e-

lectron behaves as a spectator during the ion core excitation step. The frequency for the C – H stretching mode (ν_{12}^+) of $ClCH=CCl_2^+$, which is predicted to be indiscernible in the VUV-PFI-PE measurement, has been determined to be 3073 cm^{-1} in the recent VUV-IR-PIRI study[35].

In this paper, we report a VUV-PFI-PE study of $ClCH=CCl_2$. Other than the determination of a precise value for the *IE*($ClCH=CCl_2$), the VUV-PFI-PE vibrational bands in the frequency region of 0 ~ 3250 cm^{-1} above the *IE*($ClCH=CCl_2$) have been assigned with the aid of FCF calculations. The assignment allows the determination of eleven fundamental vibrational frequencies of $ClCH=CCl_2^+$ in the ground electronic state. Combining the results of VUV-PFI-PE and VUV-IR-PIRI studies, we have determined a complete set of frequencies for the twelve vibrational modes of $ClCH=CCl_2^+$.

2 Experimental and theoretical considerations

2.1 VUV-PIE and VUV-PFI-PE measurements

The VUV laser photoion-photoelectron apparatus has been described in previous studies[29,30]. In this experiment, the VUV laser radiation is generated via nonlinear four-wave difference-frequency mixings in a Kr gas cell. The gas cell is equipped with a fused silica entrance window and a MgF_2 exit window. The Kr pressure used in the gas cell is ≈0.8 kPa. The UV frequency ω_1 is fixed at 47061.831 cm^{-1} (212.49 nm) to match the two-photon resonance of the Kr 4p → 5p transition at 94093.66 cm^{-1}. This 212.49 nm light pulse is generated by frequency-doubling of the 425 nm output of a dye laser (Laser Analytical System, LDL 20505), which is pumped by the 355 nm output of an injection seeded Nd∶YAG laser (Spectra-Physics, GCR-290) operated at 30 Hz. The second dye laser (Laser Analytical System, LDL 20505), pumped either by the 355 or 532 nm output of the same Nd∶YAG laser, is tuned to give the desired visible frequency ω_2. The UV and visible light pulses are merged via a dichroic mirror and focused (focal length = 30 cm) into the Kr gas cell. The resulting VUV ($2\omega_1 - \omega_2$) light is separated from the UV and visible fundamental lights via a windowless VUV monochromator (McPherson model 343). The monochromator also serves to focus the VUV light on the photoionization region. The VUV light intersects the sample beam in the photoionization region at 90°, where ions and electrons are produced. After passing through the photoionization region, the VUV beam is intercepted by a copper photoelectric detector for monitoring the VUV light intensities. During the experiment, the output of ω_2 is continuously monitored by a wavemeter (Coherent WaveMaster) for the purpose of frequency calibration.

The trichloroethene sample was purchased from Aldrich (>99.5% purity) and used without further purification. The gaseous sample was introduced into the photoionization region of the photoion-photoelectron apparatus in the form of a skimmed supersonic beam. The trichloroethene vapor was premixed with helium to a total stagnation pressure of 152 kPa in a liquid trichloroethene sample container prior to expansion through a pulsed valve (nozzle diameter = 0.5 mm, repetition rate = 30 Hz). The sample container was maintained at ≈0℃ using an ice-water bath. The beam source chamber and the photoionization chamber were evacuated by a 10" water-cooled diffusion pump (nominal pumping speed = 5000 L/s) and two turbomolecular pumps (pumping speed = 600 L/s each) and were maintained at pressures of 1.33 and 0.013 mPa, respectively, during the experiment.

The electron TOF detector and the ion TOF detector are situated below and above the photoionization region with the electron, respectively with the electron and ion TOF axes perpendicular to the VUV and molecular beams. For PFI-PE measurements, a dc field of ≤0.2 V/cm is applied to the photoionization region for dispersing the prompt background electrons away from the electron multichannel plate (MCP) detector. After a delay of ≈3 μs with respect to the firing of the VUV laser, a PFI field of 0.3 V/cm (width = 100 ns) is applied to the photoionization region for field ionization of high-*n* Rydberg molecules prepared by VUV excitation. This PFI field also serves to extract PFI-PEs

toward the electron MCP detector. Under the PFI conditions described above, the Stark shift for PFI-PE measurements has been shown to be governed by the relation, $4.1\sqrt{F}$ cm^{-1}, where F is the amplitude of the PFI pulse in V/cm[30]. The energy scales for all the PFI-PE spectra presented here have been corrected according to this relation. For PIE measurements, a dc field of 6 V/cm is applied to the photoionization region to extract the ions toward the ion TOF tube, which are subsequently detected by the ion MCP.

The timing sequence for opening of the pulsed valve, firing of the Nd:YAG laser, and applying the PFI field is controlled by two digital delay units (Stanford Research DG535). The signal from the electron (or ion) MCP is pre-amplified before feeding into a boxcar integrator (Stanford Research SR250). The signal from the VUV light detector is fed into another boxcar integrator. Both boxcar integrators are interfaced to a personal computer, which also controls the scanning of the dye lasers. The PIE and PFI-PE spectra presented here have been normalized by the corresponding VUV light intensities.

2.2 Theorectical calculations

Ab initio calculations have been performed on $ClCH=CCl_2^+$ with the GAUSSIAN 03 (G03) package of programs[36]. The Guassian-3X (G3X) method[37] was employed to calculate the adiabatic *IE* ($ClCH=CCl_2$). We have also carried out high-level ab initio calculations involving the approximation to complete basis set (CBS) energies at the couple cluster level with single, double, and quasi-perturbative triple excitations included (CCSD(T,Full)/CBS). The geometry optimizations and harmonic vibrational frequencies are first calculated at the B3LYP/aug-cc-pV(T+d)Z/cc-pVTZ (the standard cc-pVTZ basis sets were used on H and C and the aug-cc-pV(T+d)Z basis set was used on Cl)[38] level of theory using the G03 program package. With the optimized geometry, single point energy calculations are carried out at CCSD(T)/aug-cc-pV(x+d)Z/cc-pVxZ (x = D, T, and Q) levels. The CBS energies are then estimated by a mixed exponent/Guassian function of the form[39]

$$E(x) = E_{CBS} + B\exp[-(x-1)] + C\exp[-(x-1)^2] \quad (1)$$

where $x=2$, 3, and 4 for cc-pVDZ, cc-pVTZ, and cc-pVQZ, respectively. The zero-point vibrational energy corrections for $ClCH=CCl_2$/$ClCH=Cl_2^+$ are scaled with the factors of 0.992 and 0.971 respectively.

These scaling factors are determined by comparing the experimental[40] and calculated vibrational frequencies of neutral $ClCH=CCl_2$. The core-valence electrons correlation contributions are obtained at the CCSD(T) level using the aug-cc-pCVTZ basis set[41]. The scalar relativistic effect is computed at ACPF/MT small level[42]. In the core-valence and scalar relativistic calculations, the 1s electrons of Cl are uncorrelated throughout. All CBS energy calculations and correlation contributions are preformed using the MOLPRO 2002.6 program suit[43].

To assist the assignment on the vibrational bands resolved in VUV-PFI-PE spectra, FCF simulations are performed using the momoFCF program[44,45]. With the optimized geometries, vibrational frequencies, and normal mode displacement vectors obtained with the G03 program package, the mono FCF program is employed to calculate the overlap integrals between the vibrational wavefunctions of neutral and cationic states. The program has assumed that the potential energy surfaces of both states are harmonic and have taken into account the Duschinsky effect. In our study, the simulations are based on the optimized geometries and vibrational frequencies at the MP2(Full)/6-311G(2df,p) and B3LYP/aug-cc-pV(T+d)Z/cc-pVTZ levels of theory. The frequencies scaling factors used for $ClCH=CCl_2$/$ClCH=CCl_2^+$ are 0.971 at MP2 and 0.992 at B3LYP. Because of the weak intensities in the higher order overtones with more than 5 quanta, we have limited the number of transitions involved in the simulations. The allowed vibrational transitions are from $ClCH=CCl_2(v_1=0, v_2=0, \cdots, v_{12}=0) \rightarrow CH_3CH=CCl_2^+(v_1^+=x_1, v_2^+=x_2, \cdots, v_{12}^+=x_{12})$, where individual x_i ($i=1\sim12$) values can be any integer from 1 to 5.

We have also calculated the rotational constants

for $ClCH=CCl_2/ClCH=CCl_2^+$ at the MP2(Full)/6-311G(2df,p) level of theory. These constants are used in the spectral simulation of the origin VUV-PFI-PE vibrational band of $ClCH=CCl_2^+$. Table 1 displays the calculated rotational constants and the corresponding geometrical parameters (bond lengths r, bond angles $\angle$) for $ClCH=CCl_2$ and $ClCH=CCl_2^+$.

Table 1 Calculated rotational constants A/A^+, B/B^+, and C/C^+, bond length, bond angles for $ClCH=CCl_2/ClCH=CCl_2^+$ at the MP2(Full)/6-311G(2df,p) level of theory

	$ClCH=CCl_2$	$ClCH=CCl_2^+$	△(ion-neutral) *
Rotational constants/cm^{-1}			
A/A^+	0.132	0.133	0.001
B/B^+	0.051	0.054	0.003
C/C^+	0.037	0.038	0.001
Bond length/Å			
$r(C_2-Cl_3)$	1.715	1.655	−0.060
$r(C_2-Cl_4)$	1.703	1.651	−0.052
$r(C_1-Cl_5)$	1.705	1.630	−0.075
$r(C_1=C_2)$	1.334	1.408	0.074
$r(C_1-H)$	1.081	1.086	0.005
Bond angles/(°)			
$\angle(H-C_1-C_2)$	120.4	119.0	−1.0
$\angle(C_1-C_2-Cl_3)$	120.0	117.7	−2.3
$\angle(C_1-C_2-Cl_4)$	124.0	122.2	−1.8
$\angle(C_2-C_1-Cl_5)$	123.7	123.2	−0.5

* The difference between the value for the neutral and that for the ion.

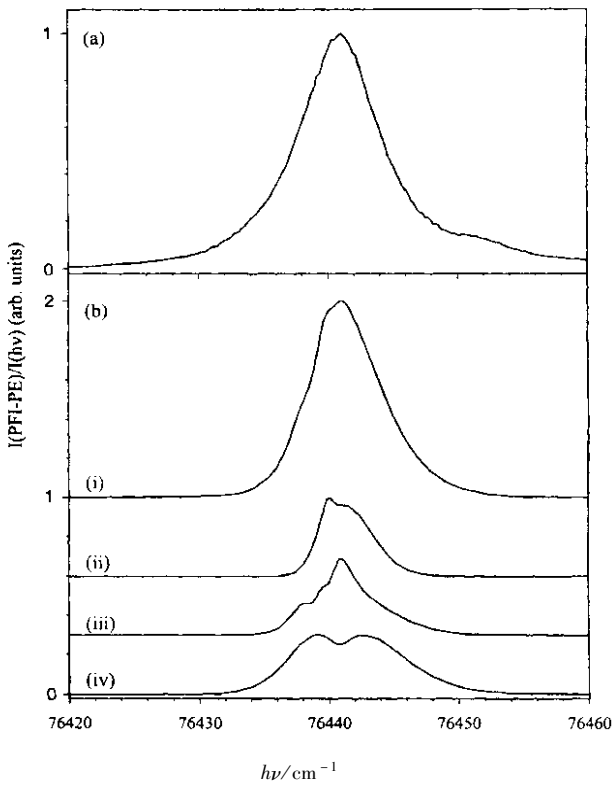

Fig. 1 (a) The origin VUV-PFI-PE vibrational band for $ClCH=CCl_2^+$ in the energy range of 76 420 ~ 76 460 cm^{-1}; (b) (i) represents the best simulated spectrum for origin VUV-PFI-PE vibrational band for $ClCH=CCl_2^+$ obtained by using a rotational temperature of 30 K and a Gaussian width of 1 cm^{-1}; (ii), (iii) and (iv) are the contributions by the Q branches ($\Delta J=0$, $\Delta K=0,\pm1$), the P plus R branches ($\Delta J=\pm1$, $\Delta K=0,\pm1$), and other branches (($\Delta J=0,\pm1$; $\Delta K=\pm2$) plus ($\Delta J=\pm2$; $\Delta K=0,\pm1,\pm2$)), respectively.

3 Results and discussion

3.1 Simulation of the origin VUV-PFI-PE vibrational band

Figure 1 (a) depicts the origin VUV-PFI-PE vibrational band for $ClCH=CCl_2^+$. The FWHM observed for this band is about 8 ~ 10 cm^{-1}. In order to obtain a more precise $IE(ClCH=CCl_2)$ value, we have performed a simulation of the origin band using the semi-empirical scheme as described in previous studies. The simulation is performed using a rotational temperature of 30 K and a Gaussian linewidth of 1 cm^{-1}. Curve (i) of Fig. 2(b) represents the best simulated spectrum, whereas its contributions from the Q-branch, P- plus R-branches, and other rotational branches are shown as curves (ii), (iii), and (iv) of Fig. 2(b), respectively. Relative intensities of curves (ii), (iii), and (iv) show that the contributions from the individual rotational branches are similar. The maximum intensities of both spectra of Fig. 2(a) and curve (i) of Fig. 2(b) have been normalized to 1 for the comparison purpose. Although the spectrum of Fig. 2(a) is nearly structure less, the simulation still serves to identify the Q-branch transitions, which in turn give the $IE(ClCH=CCl_2)$ value of (76441.7 ± 2.0) cm^{-1} (9.47764 ± 0.00025 eV). This latter value is consistent with those obtained in previous PIE and HeI photo-

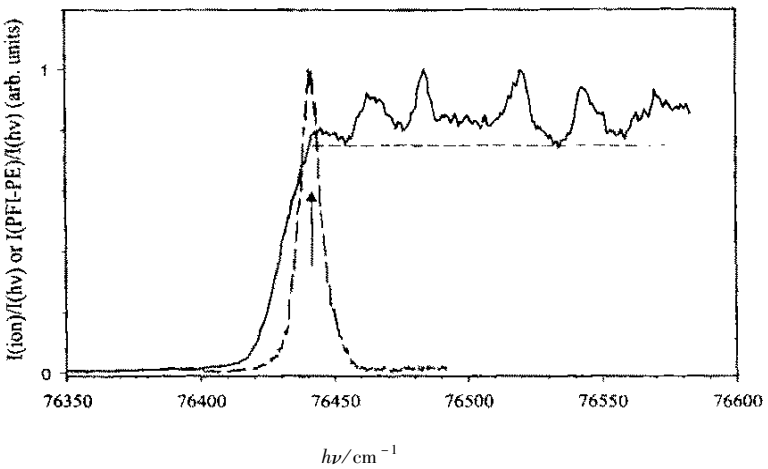

Fig. 2　Comparison of the VUV-PIE and the VUV-PFI-PE origin vibrational band of $ClCH=CCl_2$

The dashed line represents the estimation the PIE plateau due to direct photoionization.
That is, the weak peaks above the dashed line are attributed to autoionization structures.
The arrow marked the lowest energy at which the PIE reached the top of the PIE step or plateau.
This energy is coincide with the peak of the Peak of the origin vibrational band,
which marks the *IE*($ClCH=CCl_2$).

electron measurements[12]. The theoretical calculations based on the CCSD(T, Full)/CBS and G3X procedures yield *IE* values of 9.48 and 9.46 eV respectively, which are also in good accord with the value determined in this study.

3.2　Comparison of the VUV-PIE spectrum and the origin VUV-PFI-PE vibrational band

Since it is easier to obtain a PIE spectrum than a photoelectron spectrum, most of *IE* values for molecules reported previously are determined based on PIE measurements. The threshold law for direct photoionization predicts a step function behavior for the PIE onset. Due to the hot band effect, photoions can be formed at energies below the true *IE*, giving rise to a tailing structure toward lower energies. For gas samples with known temperatures, the rotational hot band structure can be simulated assuming a Boltzmann distribution for the rotational excitation. Such a simulation of the PIE onset would yield a more reliable *IE* value for the sample molecule. In order to lower the hot band effect, the supersonic beam method is often used to introduce the gas sample into the photoionization region. In such experiments, the rotational temperature of ≈ 30 K can be readily achieved for simple polyatomic species. However, the hot tail structure remains substantial for polyatomic molecules at a rotational temperature of 30 K. The simulation of the hot band tailing structure can be complicated by the accidental superposition of autoionizing resonances and by the Stark ionization due to a finite repeller field used for the ion extraction. Furthermore, thermal excitations of the low frequency torsional modes are possible for polyatomic species. This, together with the fact that photoionization cross sections for vibrationally excited molecules are not known, could make the simulation of the PIE onset difficult.

Partly because of these difficulties, most *IE* values for polyatomic species reported in the literature, particularly those determined based on PIE measurements, are subject to a significant uncertainty. It would be useful to identify a distinct feature in the PIE measurement, which is of physical significance, for a proper assignment of the *IE* value. In recent VUV-PIE and VUV-PFI-PE studies of *cis*- and *trans*-2-butenes and *cis*- and *trans*-1-bromopropenes, we find that the *IE* value determined by the VUV-PFI-PE spectrum is in excellent agreement with the lowest energy at which the PIE reaches its plateau value, i. e., the top of the PIE step after correcting for the contribution from autoionization. This observation is consistent with the argu-

ment that all molecules, including the molecules in the ground state would ionize at the true *IE*. Since the PIE at a given energy measures the sum of all the photoion intensities, the PIE is expected to reach the top or plateau of the PIE step at the true *IE* value.

Figure 2 compares the VUV-PIE spectrum for $ClCH=CCl_2$ with the origin VUV-PFI-PE vibrational band for $ClCH=Cl_2^+$. The simulation described above indicates that the *IE* ($ClCH=CCl_2$) can be reliably identified by the peak of the origin VUV-PFI-PE vbrational band. The horizontal dashed line of Fig. 2 shows the plateau or top of the PIE step due to direct photoionization. The small peaklike structures are attributed to autoionization. The lowest energy at which the PIE reaches the top of the step is marked by the arrow in Fig. 2. In accord with the observation of previous comparisons, we find here that this lowest energy indicated by the arrow coincides with the peak of the origin band. Thus, we conclude that the lowest energy at which the PIE reaches its plateau value is the distinct feature that can be used for a reliable *IE* assignment. However, we emphasize that more precise *IE* values can usually be obtained by PFI-PE measurements than by PIE measurements. Thus, when the PFI-PE spectrum is available, its use for the *IE* determination should be preferred.

3.3 The FCF simulation and vibrational assignment of the VUV-PFI-PE spectrum

The $ClCH=CCl_2^+$ cation has twelve fundamental vibrational modes. The scaled harmonic vibrational frequencies calculated at the DFT and MP2 levels of theory are listed in Table 2. These frequencies are arranged in the increasing order with labels from ν_1^+ to ν_{12}^+. As shown in this table, the theoretical DFT and MP2 frequencies are in close agreement except those for ν_8^+, where the deviation between the DFT and MP2 predictions is more than 50 cm^{-1}.

The VUV-PFI-PE spectra for $ClCH=CCl_2$ recorded in the present study are plotted in Figs. 3(a) and 4(a), whereas the corresponding FCF simulation spectra are shown in Figs. 3(b) and 4(b). The origin vibrational bands of Figs. 3(a) and (b) have been normalized to unity for the comparison purpose. We note that the intensity scales for Figs. 3 and 4 are identical. Table 3 summarizes the assignments of the VUV-PFI-PE bands resolved in the spectra of Figs. 3(a) and 4(a) based on their comparison with the theoretical frequencies and relative FCFs, which are also given in Table 3.

The ground vibrational state for the neutral $ClCH=CCl_2$ has a′ symmetry. Thus, the FCF photoionization transition is expected to favor the formation of vibrational states for $ClCH=CCl_2^+$ with a′ symmetry. This expectation is consistent with the calculated FCFs. With this expectation in mind, it is relatively straight forward to assign the VUV-PFI-PE peaks at 286, 300, 402, 565, 660, 687, 806, 947, 990, 1038, 1064, 1091, 1230, 1267, 1287, 1321, 1340, 1351, and 1408 cm^{-1} to be ν_3^+, $2\nu_1^+$, ν_4^+, $2\nu_3^+$, ν_6^+, $(\nu_3^+ + \nu_4^+)$, $2\nu_4^+$, $(\nu_3^+ + \nu_6^+)$, ν_8^+, ν_9^+, $(\nu_4^+ + \nu_6^+)$, $(\nu_3^+ + 2\nu_4^+)$, $(2\nu_3^+ + \nu_6^+)$, ν_{10}^+, $(\nu_3^+ + \nu_8^+)$, $2\nu_6^+$, $(\nu_3^+ + \nu_9^+)$, $(\nu_3^+ + \nu_4^+ + \nu_6^+)$,

Table 2 Theoretical and experimental vibrational frequencies for $ClCH=CCl_2^+$

Vibrational mode (Symmetry)	Theoretical[a] DFT/MP2/cm^{-1}	VUV – PFI-PE[b] /cm^{-1}
ν_1^+ (a″)	148/152	148
ν_2^+ (a′)	180/179	180
ν_3^+ (a′)	290/291	286
ν_4^+ (a′)	402/405	402
ν_5^+ (a″)	476/487	472
ν_6^+ (a′)	654/664	660
ν_7^+ (a″)	824/839	875
ν_8^+ (a′)	931/983	990
ν_9^+ (a′)	1012/1051	1038
ν_{10}^+ (a′)	1283/1275	1267
ν_{11}^+ (a′)	1403/1413	1408
ν_{12}^+ (a′)	3163/3124	3073[c]

a. Theoretical vibrational frequencies are scaled from harmonic frequencies using factors of 0.992 and 0.971 for $ClCH=CCl_2$ at B3LYP/aug-cc-pV(T+d)Z/cc-pVTZ (DFT) and MP2(Full)/6-311G(2df,p), respectively.

b. This work. Experimental values obtained based on the assignment of vibrational bands resolved in the VUV-PFI-PE spectrum.

c. Reference [35].

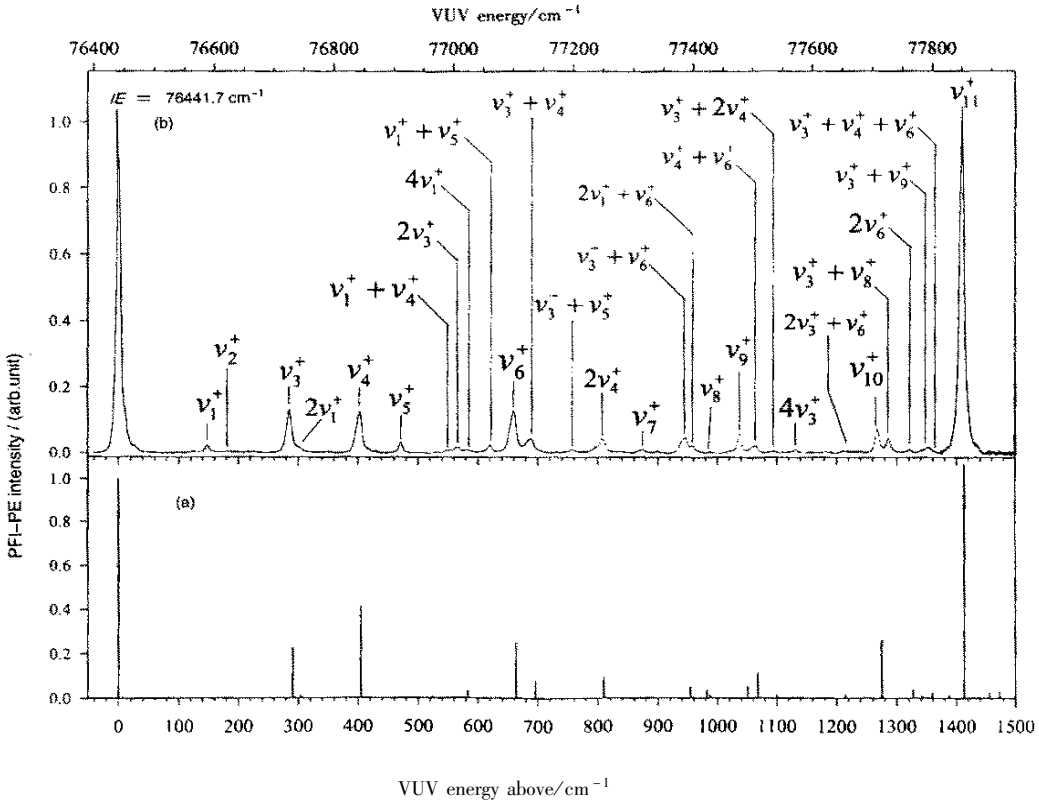

Fig. 3　(a) VUV-PFI-PE spectrum of $ClCH=CCl_2$ in the energy range of 0 ~ 1500 cm^{-1} above $IE(ClCH=CCl_2)$, (b) The FCF simulated spectrum in the same energy range as that in (a).

and ν_{11}^+, respectively, which all have a′ symmetry. All the above-mentioned peaks have frequencies and relative intensities comparable to the FCF predictions. Several predicted low intensities a′ peaks are also observed, while the bands at 180, 584, 621, 956 and 1132 cm^{-1} are assigned as ν_2^+, $4\nu_1^+$, $(\nu_1^+ + \nu_5^+)$, $(2\nu_1^+ + \nu_6^+)$, and $4\nu_3^+$ respectively. The relative intensities of these vibrationl bands are predicted to be low (< 0.005), but they are still discernible in the PFI-PE spectrum. Although vibrational bands for $ClCH=CCl_2^+$ with a″ symmetry are not predicted by the FCF calculation, several a″ transitions are observed. The first peak at 148 cm^{-1} is a case in point, and this peak is best assigned as the ν_1^+ mode (a″). Similar arguments are also applied to the peaks at 472, 553, 758, and 875 cm^{-1}, which are assigned as ν_5^+, $(\nu_1^+ + \nu_4^+)$, $(\nu_3^+ + \nu_5^+)$, and ν_7^+. There are several a′ transitions, which are predicted by the FCF, but not observed in the VUV-PFI-PE spectrum, and which are also listed in Table 3. Their expected experimental values are in parentheses in column two of Table 3. We note that based on the above assignment, the fundamental vibrational frequencies for the eleven vibrational modes from ν_1^+ to ν_{11}^+ are determined.

In the frequency region of 1500 ~ 3200 cm^{-1} above the IE($ClCH=CCl_2$), it is expected that most of the vibrational peaks are due to combination bands or overtones involving ν_1^+ to ν_{11}^+. Similar to the frequency region of 0 ~ 1500 cm^{-1}, we first assign the a′ vibrational bands that matches the predictions of the FCF simulation. The VUV-PFI-PE peaks observed at 1553, 1603, 1668, 1692, 1810, 1834, 1925, 1958, 1973, 2066, 2091, 2212, 2267, 2301, 2349, 2442, 2465, 2529, 2662, 2685, 2720, 2748, 2798, 2941, 2967, 3005, 3075, and 3194 cm^{-1} are assigned as $(\nu_3^+ + \nu_{10}^+)$, $(\nu_3^+ + 2\nu_6^+)$, $(\nu_4^+ + \nu_{10}^+)$, $(\nu_3^+ + \nu_{11}^+)$, $(\nu_4^+ + \nu_{11}^+)$, $(2\nu_3^+ + \nu_{10}^+)$, $(\nu_6^+ + \nu_{10}^+)$, $(\nu_3^+ +$

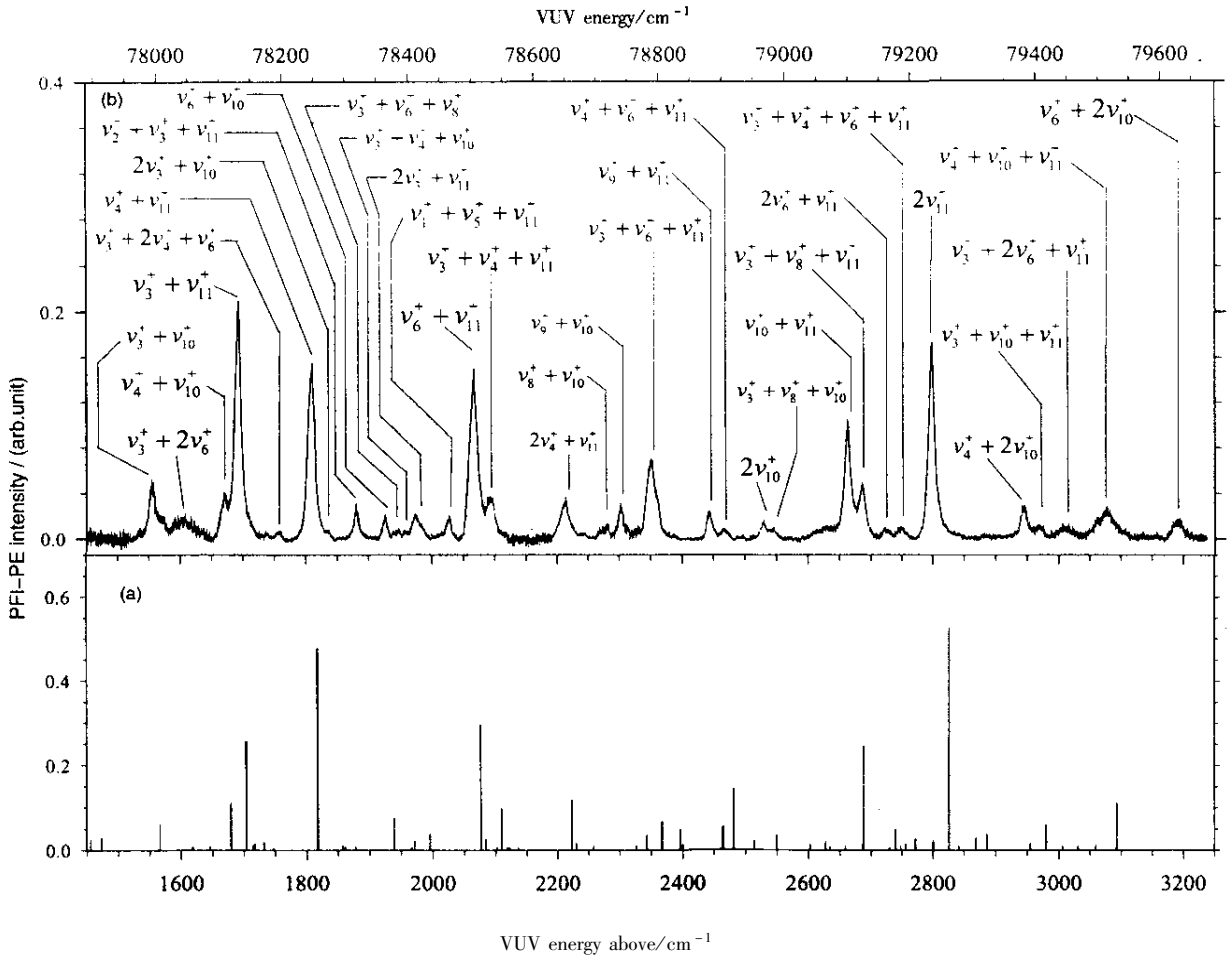

Fig. 4 (a) VUV-PFI-PE spectrum of $ClCH=CCl_2$ in the energy range of 1500 ~ 3200 cm^{-1} above $IE(ClCH=CCl_2)$. (b) The FCF simulated spectrum in the same energy range as that in (a).

$\nu_4^+ + \nu_{10}^+$), ($2\nu_3^+ + \nu_{11}^+$), ($\nu_6^+ + \nu_{11}^+$), ($\nu_3^+ + \nu_4^+ + \nu_{11}^+$), ($2\nu_4^+ + \nu_{11}^+$), ($\nu_8^+ + \nu_{10}^+$), ($\nu_9^+ + \nu_{10}^+$), ($\nu_3^+ + \nu_6^+ + \nu_{11}^+$), ($\nu_9^+ + \nu_{11}^+$), ($\nu_4^+ + \nu_6^+ + \nu_{11}^+$), $2\nu_{10}^+$, ($\nu_{10}^+ + \nu_{11}^+$), ($\nu_3^+ + \nu_8^+ + \nu_{11}^+$), ($2\nu_6^+ + \nu_{11}^+$), ($\nu_3^+ + \nu_4^+ + \nu_6^+ + \nu_{11}^+$), $2\nu_{11}^+$, ($\nu_4^+ + 2\nu_{10}^+$), ($\nu_3^+ + \nu_{10}^+ + \nu_{11}^+$), ($\nu_3^+ + 2\nu_6^+ + \nu_{11}^+$), ($\nu_4^+ + \nu_{10}^+ + \nu_{11}^+$), and ($\nu_6^+ + 2\nu_{10}^+$), respectively. For the remaining five VUV-PFI-PE peaks at 1775, 1879, 1945, 2026, and 2544 cm^{-1}, although their relative intensities have larger discrepancies with the FCF predictions, their positions are best matched with ($\nu_3^+ + 2\nu_4^+ + \nu_6^+$), ($\nu_2^+ + \nu_3^+ + \nu_{11}^+$), ($\nu_4^+ + \nu_6^+ + \nu_8^+$), ($\nu_1^+ + \nu_5^+ + \nu_{11}^+$), and ($\nu_3^+ + \nu_8^+ + \nu_{10}^+$), respectively. With the aid of FCF calculations, all the VUV-PFI-PE vibrational bands in this energy region are satisfactorily assigned to vibrational states with a′ symmetry.

The experimental frequencies for the eleven vibrational modes ν_1^+ to ν_{11}^+ determined in the present VUV-PFI-PE study, together with the ν_{12}^+ frequency, determined in the previous VUV-IR-PIRI measurement[35], are summarized in Table 2 for comparison with the theoretical MPT and DFT frequencies.

3.3 Excitation of the ν_{11}^+ and ν_{12}^+ modes

One of the distinct features of the VUV-PFI-PE spectrum is the observation of the extremely strong $\nu_{11}^+ = 1$ vibrational band and the absence of the $\nu_{12}^+ = 1$ vibrational band. Aside from the FCF calculation, this observation can be explained by the geometrical change of $ClCH=CCl_2$ upon photoionization. As shown in Table 1, the largest change between the cation and

Table 3　Comparison between theoretical frequencies and relative FCF intensities and experimental frequencies and relative intensities for VUV-PFI-PE vibrational bands for $ClCH=CCl_2^+$

Assignment (symmetry)	VUV-PFI-PE[a]		FCF calculation[b]	
	Frequencies/cm^{-1}	Relative intensities[c]	DFT/MP2 frequencies/cm^{-1}[d]	Relative intensities[c]
ν_1^+ (a″)	148	0.0247	148/152	—
ν_2^+ (a′)	180	0.0059	180/179	0.0020
ν_3^+ (a′)	286	0.1346	290/291	0.2273
$2\nu_1^+$ (a′)	300	0.0209	296/304	0.0129
ν_4^+ (a′)	402	0.1287	402/405	0.4154
ν_5^+ (a″)	472	0.0338	476/487	—
$\nu_1^+ + \nu_4^+$ (a″)	553	0.0100	550/557	—
$2\nu_3^+$ (a′)	565	0.0181	580/582	0.0326
$4\nu_1^+$ (a′)	584	0.0093	592/608	0.0003
$\nu_1^+ + \nu_5^+$ (a′)	621	0.0237	624/639	0.0041
ν_6^+ (a′)	660	0.1303	654/664	0.2496
$\nu_3^+ + \nu_4^+$ (a′)	687	0.0446	692/696	0.0814
$2\nu_1^+ + \nu_4^+$ (a′)	(698)	—	698/709	0.0054
$\nu_3^+ + \nu_5^+$ (a″)	758	0.0116	766/778	—
$2\nu_4^+$ (a′)	806	0.0437	804/810	0.0970
ν_7^+ (a″)	875	0.0126	824/839	—
$\nu_3^+ + \nu_6^+$ (a′)	947	0.0478	944/955	0.0532
$2\nu_1^+ + \nu_6^+$ (a′)	956	0.0236	950/968	0.0039
ν_8^+ (a′)	990	0.0025	931/983	0.0351
$2\nu_3^+ + \nu_4^+$ (a′)	(974)	—	982/987	0.0103
ν_9^+ (a′)	1038	0.0588	1012/1051	0.0503
$\nu_4^+ + \nu_6^+$ (a′)	1064	0.0234	1056/1069	0.1162
$\nu_3^+ + 2\nu_4^+$ (a′)	1091	0.0047	1094/1101	0.0165
$4\nu_3^+$ (a′)	1132	0.0114	1160/1164	0.0003
$3\nu_4^+$ (a′)	(1206)	—	1206/1215	0.0167
$2\nu_3^+ + \nu_6^+$ (a′)	1230	0.0062	1234/1246	0.0072
ν_{10}^+ (a′)	1267	0.0755	1283/1275	0.2606
$\nu_3^+ + \nu_8^+$ (a′)	1287	0.0470	1221/1274	0.0108
$2\nu_6^+$ (a′)	1321	0.0123	1308/1328	0.0376
$\nu_3^+ + \nu_9^+$ (a′)	1340	0.0093	1302/1342	0.0119
$\nu_3^+ + \nu_4^+ + \nu_6^+$ (a′)	1351	0.0178	1346/1360	0.0215
ν_{11}^+ (a′)	1408	0.9985	1403/1413	1.0690
$\nu_4^+ + \nu_9^+$ (a′)	(1440)	—	1414/1456	0.0246
$2\nu_4^+ + \nu_6^+$ (a′)	(1464)	—	1458/1474	0.0299
$\nu_3^+ + \nu_{10}^+$ (a′)	1553	0.0108	1573/1566	0.0599
$\nu_3^+ + 2\nu_6^+$ (a′)	1603	0.0232	1598/1619	0.0076
$\nu_4^+ + \nu_{10}^+$ (a′)	1668	0.0414	1685/1680	0.1102
$\nu_3^+ + \nu_{11}^+$ (a′)	1692	0.2111	1693/1704	0.2563

Continued on Table 3.

Assignment (symmetry)	VUV-PFI-PE[a]		FCF calculation[b]	
	Frequencies/cm^{-1}	Relative intensities[c]	DFT/MP2 frequencies/cm^{-1}[d]	Relative intensities[c]
$\nu_3^+ + 2\nu_4^+ + \nu_6^+$ (a′)	1757	0.0066	1748/1765	0.0053
$\nu_4^+ + \nu_{11}^+$ (a′)	1810	0.1558	1805/1818	0.4768
$2\nu_3^+ + \nu_{10}^+$ (a′)	1834	0.0083	1863/1857	0.0086
$\nu_2^+ + \nu_3^+ + \nu_{11}^+$ (a′)	1879	0.0312	1873/1883	0.0010
$\nu_6^+ + \nu_{10}^+$ (a′)	1925	0.0215	1937/1939	0.0761
$\nu_3^+ + \nu_6^+ + \nu_8^+$ (a′)	1945	0.0092	1875/1938	0.0015
$\nu_3^+ + \nu_4^+ + \nu_{10}^+$ (a′)	1958	0.0055	1975/1971	0.0219
$2\nu_3^+ + \nu_{11}^+$ (a′)	1973	0.0220	1983/1995	0.0382
$\nu_1^+ + \nu_5^+ + \nu_{11}^+$ (a′)	2026	0.0211	2027/2052	0.0040
$\nu_6^+ + \nu_{11}^+$ (a′)	2066	0.1603	2057/2077	0.2965
$\nu_3^+ + \nu_4^+ + \nu_{11}^+$ (a′)	2091	0.0386	2095/2109	0.0992
$2\nu_4^+ + \nu_{11}^+$ (a′)	2212	0.0366	2207/2223	0.1184
$\nu_8^+ + \nu_{10}^+$ (a′)	2267	0.0108	2214/2258	0.0094
$\nu_9^+ + \nu_{10}^+$ (a′)	2301	0.0324	2295/2236	0.0101
$\nu_3^+ + \nu_6^+ + \nu_{11}^+$ (a′)	2349	0.0727	2347/2368	0.0668
$\nu_9^+ + \nu_{11}^+$ (a′)	2442	0.0245	2415/2464	0.0552
$\nu_4^+ + \nu_6^+ + \nu_{11}^+$ (a′)	2465	0.0087	2459/2482	0.1463
$2\nu_{10}^+$ (a′)	2529	0.0175	2566/2550	0.0357
$\nu_3^+ + \nu_8^+ + \nu 10 +$ (a′)	2544	0.0101	2563/2577	0.0030
$\nu 10 + + \nu_{11}^+$ (a′)	2662	0.1059	2686/2688	0.2462
$\nu_3^+ + \nu_8^+ + \nu_{11}^+$ (a′)	2685	0.0498	2624/2687	0.0150
$2\nu_6^+ + \nu_{11}^+$ (a′)	2720	0.0106	2711/2714	0.0485
$\nu_3^+ + \nu_4^+ + \nu_6^+ + \nu_{11}^+$ (a′)	2748	0.0120	2749/2773	0.0208
$2\nu_{11}^+$ (a′)	2798	0.1761	2806/2826	0.5253
$\nu_4^+ + 2\nu_{10}^+$ (a′)	2941	0.0305	2968/2955	0.0153
$\nu_3^+ + \nu_{10}^+ + \nu_{11}^+$ (a′)	2967	0.0132	2976/2979	0.0599
$\nu_3^+ + 2\nu_6^+ + \nu_{11}^+$ (a′)	3005	0.0139	3110/3032	0.0104
$\nu_4^+ + \nu_{10}^+ + \nu_{11}^+$ (a′)	3075	0.0309	3088/3093	0.1123
$\nu_3^+ + 2\nu_{11}^+$ (a′)	(3102)	—	3096/3117	0.1332
ν_{12}^+ (a′)	—	—	3163/3131	0.0003
$\nu_6^+ + 2\nu_{10}^+$ (a′)	3194	0.0181	3220/3214	0.1197

a. Experimental frequencies and relative intensities for PFI – PE vibrational bands observed in the VUV-PFI-PE spectrum for $ClCH=CCl_2$.

b. Caclulated FCFs using the momoFCF program (Ref. [34]).

c. The relative intensities for the origin vibrational band is arbitrarily normalized to unity.

d. Calculated theoretical frequencies of Table 2.

neutral are in the bond lengths of r(C – Cl) and r(C=C), suggesting that the C – Cl and C=C stretching mode is preferentially excited in the formation of $ClCH=CCl_2^+$ from $ClCH=CCl_2$. The ν_{11}^+ mode is the C=C stretching mode for r(C=C). The fact that the r(C=C) distance for $ClCH=CCl_2^+$ formed by the photoionization is significantly shorter than the equilib-

rium $r(C=C)$ explains the very strong intensity for the ν_{11}^+ band observed in the VUV-PFI-PE spectrum. Similarly, owing to the small change in the $r(C-H)$ distance upon photoionization, excitation of the ν_{12}^+ ($C-H$ stretch) mode of $ClCH=CCl_2^+$ should be negligible. In the FCF calculation, the relative intensity of the ν_{12}^+ mode is found to be 3×10^{-4}.

4 Conclusion

The VUV-PIE and VUV-PFI-PE spectrum of trichloroethene near the ionization threshold has been measured using tunable VUV laser radiation. The simulation of the origin VUV-PFI-PE vibrational band gives the $IE(ClCH=CCl_2)=(76\,441.7\pm2.0)\,cm^{-1}$. The vibrational bands resolved in the VUV-PFI-PE spectrum have been assigned with the aid of theoretical vibrational frequencies and calculated FCFs. The frequencies for eleven fundamental vibrational modes ν_1^+ to ν_{11}^+ of $ClCH=CCl_2^+$ are obtained from the assignment of the VUV-PFI-PE spectrum. These values, together with the ν_{12}^+ ($C-H$ stretch) frequency determined in the recent IR-PIRI study, and the complete set of twelve vibrational frequencies of $ClCH=CCl_2^+$ are obtained.

Acknowledgements: This work was supported by the U. S. Department of Energy, Office of Basic Energy Sciences, Division of Chemical Sciences, Geosciences, and Biosciences. The authors are grateful to Prof. Iwata for making available the momoFCF program and providing many helpful instructions for running the program. The calculations of this work used resources of the National Energy Research Scientific Computing Center, which is supported by the Office of Science of the U. S. Department of Energy under Contract No. DE-AC03-76SF00098. Part of the calculations was also performed using the Molecular Science Computing Facility (MSCF) in the William R. Wiley Environmental Molecular Sciences Laboratory, a national scientific user facility sponsored by the U. S. Department of Energy's Office of Biological and Environmental Research and located at the Pacific Northwest National Laboratory.

Pacific Northwest is operated for the Department of Energy by Battelle. C. Y. N. also acknowledges partial supports by the AFOSR Grant No. F49620-03-1-0116 and NSF ATM 0317422.

References

[1] Westrick J J, Mello J W, Thomas R F. *J. Am. Water Works Assoc.*, 1984, **76**: 52

[2] Russell H H, Matthews J E, Sewell G W. US Environmental Protection Agency, Office of Solid Waste and Emergency Response: Washington D. C. Issue paper EPA/540/S-92 January 1992.

[3] Donò A, Paradisi C, Scorrano G. *Rapid. Commun. Mass Spectrom.*, 1997, **11**: 1687

[4] Lash L H, Fisher J W, Lipscomb J C, Parker J C. *Environ Health Perspectives*, 2000, **108**: 177

[5] Choi J W, Tillman Jr F D, Smith J A. *Environ. Sci. Technol.*, 2002, **36**: 3157

[6] Sudb A S, Schulz P A, Grant E R, Shen Y R, Lee Y T. *J. Chem. Phys.*, 1978, **68**: 1306

[7] Reiser C, Lussier F M, Jensen C C, Steinfeld J I. *J. Am. Chem. Soc.*, 1979, **101**: 350

[8] Sudb A S, Schulz P A, Shen Y R, Lee Y T. *J. Chem. Phys.*, 1978, **69**: 2312

[9] Yokoyama K, Fujisawa G, Yokoyama A. *J. Chem. Phys.*, 1995, **102**: 7902

[10] Sato K, Tsunashima S, Takayanagi T, Fujisawa G, Yokoyama A. *J. Chem. Phys.*, 1997, **106**: 10123

[11] Lee Y J, Lee Y R, Chou C C, Lin S M. *J. Chem. Phys.*, 1998, **109**: 346

[12] The NIST Chemistry WebBook, http://webbook.nist.goc/chemistry/

[13] Müller-Dethlefs K, Sanders M, Schlag E W. *Chem. Phys. Lett.*, 1984, **112**: 291

[14] Hsu C W, Evans M, Ng C Y, Heimann P. *Rev. Sci. Instrum.*, 1997, **68**: 1694

[15] Jarvis G K, Song Y, Ng C Y. *Rev. Sci. Instrum.*, 1999, **70**: 2615

[16] Zhu L, Johnson P M. *J. Chem. Phys.*, 1991, **94**: 5769

[17] Johnson P M. *Adv. Ser. Phys. Chem.*, 1999, **10**A: 296

[18] Burrill A B, Johnson P M. *J. Chem. Phys.*, 2001, **115**: 133

[19] Jarvis G K, Weitzel K M, Malow M, Baer T, Song Y, Ng C Y. *Rev. Sci. Instrum.*, 1999, **70**: 3892

[20] Qian X M, Zhang T, Chiu Y, Levandier D J, Miller J S, Dressler R A, Ng C Y. *J. Chem. Phys.*, 2003, **118**: 2455

[21] Kung A H, Lee Y T. in Vacuum Ultraviolet Photoionization and Photodissociation of Molecules and Clusters, edited by Ng C Y. World Scientific, Singapore 1991.
[22] J. W. Hepburn in Laser Techniques in Chemistry, edited by Meyers A, Rizzo T R. Wiley, New York, 1994.
[23] Heimann P, Koike M, Hsu C W, *et al. Rev. Sci. Instrum.*, 1997, **68**: 1945
[24] Ng C Y. *Annu. Rev. Phys. Chem.*, 2002, **53**: 102
[25] A list of IE of molecules and radicals determined by PFI-PE and PFI-PI measurements can be found at the ZEKE website, http://www.zeke.org/ie.html
[26] Cheung Y S, Huang C J, Ng C Y. *J. Chem. Phys.*, 1998, **109**: 1781
[27] Cheung Y S, Hsu C W, Ng C Y, Li W K, Chiu S W. *Int. J. Mass. Spectrom. Ion Processes*, 1996, **159**: 13
[28] Cheung Y S, Ng C Y. *Int. J. Mass Spectrom. Ion Processes*, 1999, **185/186/187**: 533
[29] Woo H K, Jiping Zhan, Lau K C, Ng C Y, Cheung Y S. *J. Chem. Phys.*, 2002, **116**: 8803
[30] Woo H K, Lau K C, Jiping Zhan, Ng C Y, Li C L, Li W K, Johnson P M. *J. Chem. Phys.*, 2003, **119**: 7789
[31] Lee M, Kim M S. *J. Chem. Phys.*, 2003, **119**: 5085
[32] Lee M, Kim M S. *J. Chem. Phys.*, 2003, **119**: 12351
[33] Fujii A, Iwasaki A, Ebata T, Mikami N. *J. Phys. Chem. A*, 1997, **101**: 5963
[34] Gerhards M, Schiwek M, Unterberg C, Kleinermanns K. *Chem. Phys. Lett.*, 1998, **297**: 515
[35] Woo H K, Wang P, Lau K C, Xing X, Ng C Y. *J. Chem. Phys.*, 2004, **120**: 9561
[36] Frisch M J, Trucks G W, Schlegel H B, et al. GAUSSIAN 03, Revision B.4, Gaussian, Inc., Pittsburgh PA, 2003.
[37] Curtiss L A, Redfern P C, Raghavachari K, Pople J A. *J. Chem. Phys.*, 2001, **114**: 108
[38] (a) Dunning Jr T H, Peterson K A, Wilson A K. *J. Chem. Phys.*, 2001, **114**: 9244
(b) Dunning Jr T H. *J. Chem. Phys.*, 1989, **90**: 107
[39] Peterson K A, Woon D E, Dunning Jr T H. *J. Chem. Phys.*, 1994, **100**: 7410
[40] Mallard W G, Linstrom P J. in NIST Chemistry WebBook, Natl. Inst. Stand. Technol., Gaithersburg, MD, http://webbook.nist.gov, 1998.
[41] (a) Woon D E, Dunning Jr T H. *J. Chem. Phys.*, 1995, **103**: 4572
(b) Peterson K A, Dunnung Jr T H. *J. Chem. Phys.*, 2002, **117**: 10548
[42] Martin J M L, De Oliverira G. *J. Chem. Phys.*, 1999, **111**: 1843
[43] MOLPRO is a package of ab initio programs written by Werner H J, Knowles P J, with contributions from Amos R D, *et al.*
[44] MomoFCF program can be obtained from http://hera.ims.ac.jp.
[45] Yamaguchi M, Momose T, Shida T. *J. Chem. Phys.*, 1990, **93**: 4211